Metabolomics (2016) 12:25
DOI 10.1007/s11306-015-0936-y

ORIGINAL ARTICLE

Gut microbial activity as influenced by fiber digestion: dynamic metabolomics in an in vitro colon simulator

Santosh Lamichhane[1] · Johan A. Westerhuis[3] · Arthur C. Ouwehand[4] · Markku T. Saarinen[4] · Sofia D. Forssten[4] · Henrik Max Jensen[5] · Jette F. Young[2] · Hanne Christine Bertram[1] · Christian C. Yde[1]

Received: 12 June 2015 / Accepted: 22 October 2015 / Published online: 4 January 2016

Abstract Understanding the interaction between the gut microbial activity and the host is essential, and in vitro models are being used to test and develop hypotheses regarding the impact of food components/drugs on the human gut ecosystem. However, while in vitro models provide excellent possibilities for dynamic investigations, studies have commonly been restricted to analyses of few, targeted metabolites. In the present study, we employed NMR-based metabolomics combined with multilevel data analysis as a tool to characterize the impact of polydextrose (PDX) fiber on the in vitro derived fecal metabolome. This approach enabled us to identify and quantify the fiber-induced response on several fecal metabolites; we observed higher levels of butyrate, acetate, propionate, succinate, *N*-acetyl compound and a lower level of amino acids (leucine, valine, isoleucine, phenylalanine, and lysine), valerate, formate, isovalerate and trimethylamine among the PDX-treated sample compared to the control samples. In addition, by the application of multilevel data analysis we were able to examine the specific inter-individual variations, and caprylic acid was identified to be the main marker of distinct microbial compositions among the subjects. Our work is expected to provide a useful approach to understand the metabolic impact of potential prebiotic compounds and get deeper insight into the molecular regulation of gut-microbe activities in the complex gut system.

Keywords Nuclear magnetic resonances · Dietary fiber · Metabolomics · Gut

1 Introduction

Dietary fiber contributes to a balanced environment of the gastrointestinal tract. Intriguingly, polydextrose (PDX), a highly branched and complex polymer of glucose is classified as soluble dietary fiber by the U.S. Food and Drug Administration (FDA). In structure, PDX possesses all different combinations of 1–2, 1–3 , 1–4, and 1–6, both α- and β-glyosidic linkages, thus being resistant to hydrolysis by human digestive enzymes, passaging intact into the colon, where it is partially fermented (Lahtinen et al. 2010). In fact, fermentation of dietary fiber produces mediators such as short chain fatty acid (SCFA), organic acids, and amino acids, which might alter the microbial activities/composition in the gut and play a vital role on human health and disease (Nicholson et al. 2012; Roberfroid et al. 2010). To date, the impact of PDX intake has been investigated to some extent in human, animal models, and in in vitro colon simulator models (Achour et al. 1994; Costabile et al. 2012; Deng et al. 2014; Figdor and Rennhard 1981; Hernot et al. 2009; Hull et al. 2012;

Electronic supplementary material The online version of this article (doi:10.1007/s11306-015-0936-y) contains supplementary material, which is available to authorized users.

✉ Santosh Lamichhane
santosh.lamichhane@food.au.dk

[1] Department of Food Science, Aarhus University, Kirstinebjergvej 10, 5792 Aarslev, Denmark

[2] Department of Food Science, Aarhus University, Blichers Allé 20, 8830 Tjele, Denmark

[3] Swammerdam Institute for Life Sciences, University of Amsterdam, Science Park 904, 1098 HX Amsterdam, The Netherlands

[4] Dupont, Nutrition and Health, Sokeritehtaantie 20, 02460 Kantvik, Finland

[5] DuPont Nutrition Biosciences ApS, Edwin Rahrsvej 38, 8220 Brabrand, Aarhus, Denmark

Table 1 ^{1}H NMR chemical shifts and signal assignments of metabolites from the in vitro derived fecal material

No.	Compound	Proton chemical shift in ppm and multiplicity
1	*n*-Butyrate	0.91 (t), 1.56(t), 2.16 (t)
2	Leucine	0.96 (d), 0.97(d), 1.7 (m)
3	Isoleucine	0.94 (t), 1.02 (d), 1.27 (m)
4	Valine	0.99 (d), 1.05(d), 2.3 (m)
5	Propionate	1.06 (t), 2.19 (m)
6	Ethanol	1.18 (t), 3.6 (q)
7	Caprylate	0.85 (t), 1.27(m), 1.53 (m), 2.16(t)
8	Valerate	0.88 (t), 1.31(m), 1.54 (m), 2.18 (m)
9	Alanine	1.48 (d)
10	2-Hydroxybutyrate[a]	1.64 (m),1.72 (m)
11	Unknown	1.81 (s)
12	Acetate	1.92 (s)
13	*n*-Acetyl compound	2.02 (s)
14	Isovalerate	2.06 (d), 1.98 (m)
15	5 Aminopentonate[a]	3.02 (t), 2.21 (t), 1.69 (m)
16	Iso Butyrate	2.40 (m), 1.11 (t)
17	Succinate	2.41 (s)
18	Trimethylamine	2.87 (s)
19	Lysine	1.40 (m), 1.70 (m), 3.03 (t), 3.72 (t)
20	Methanol	3.36 (s)
21	Acetoacetate	3.41 (s) 2.32 (s)
22	*p*-Cresol	2.25 (s), 6.87 (m), 7.18(d),
23	Tyrosine	6.91 (d), 7.20 (d)
24	Tryptophan	7.19 (d), 7.31 (m), 7.76 (d)
25	Phenylacetate	6.93 (m), 7.21 (m)
26	Phenylalanine	3.54 (s), 7.31 (m), 7.37 (m)
27	Formate	8.46 (s)
28	Histamine	7.9 (s), 7.1 (s)
29	Threonine	1.33 (d), 3.57 (d), 4.24 (m)
30	Methylamine	2.59 (s)
31	3-Phenylpropionate[a]	7.31 (m), 7.40 (m), 2.9 (t)

[a] Assigned based on the best matched signals

Mäkivuokko et al. 2007). As a result, PDX has been demonstrated to benefit the digestive health in terms of improved bowel functions and an increased production of SCFAs through colonic microbial fermentation (Costabile et al. 2012; Mäkivuokko et al. 2007). In addition, an improved digestive health is also obtained due to selective growth of beneficial bacteria (Hernot et al. 2009). However, further substantiation on the effects of PDX is required, in particular; linking gut microbial activity to the gut health is essential (Romick-Rosendale et al. 2014; Ryan et al. 2014).

In vitro models have been developed and used to test and exploit hypotheses regarding the impact of food components/drugs on the human gut system (Mills et al. 2015; Mäkivuokko et al. 2007; Pereira-Caro et al. 2015). Despite the absence of the physiological environment of the host system, the main advantages of in vitro models involve the dynamic sampling possibility and less extensive use of animals or humans for research purposes. Importantly, in vitro models barely present ethical issues, and in the past, in vitro models have been extensively applied to study the microbial composition and activity (Hernot et al. 2009; Mäkivuokko et al. 2007; Pereira-Caro et al. 2015). Based on their results the in vitro model has been shown representative of in vivo situation in terms of microbial composition and activity. However, untargeted metabolic profiling to examine the effects of dietary fiber in in vitro models has been rarely reported. This is despite the fact that such an approach potentially could increase the understanding of the complete set of metabolites produced by the gut microbiota. Furthermore, it may contribute to the identification of novel biomarkers or metabolic profiles

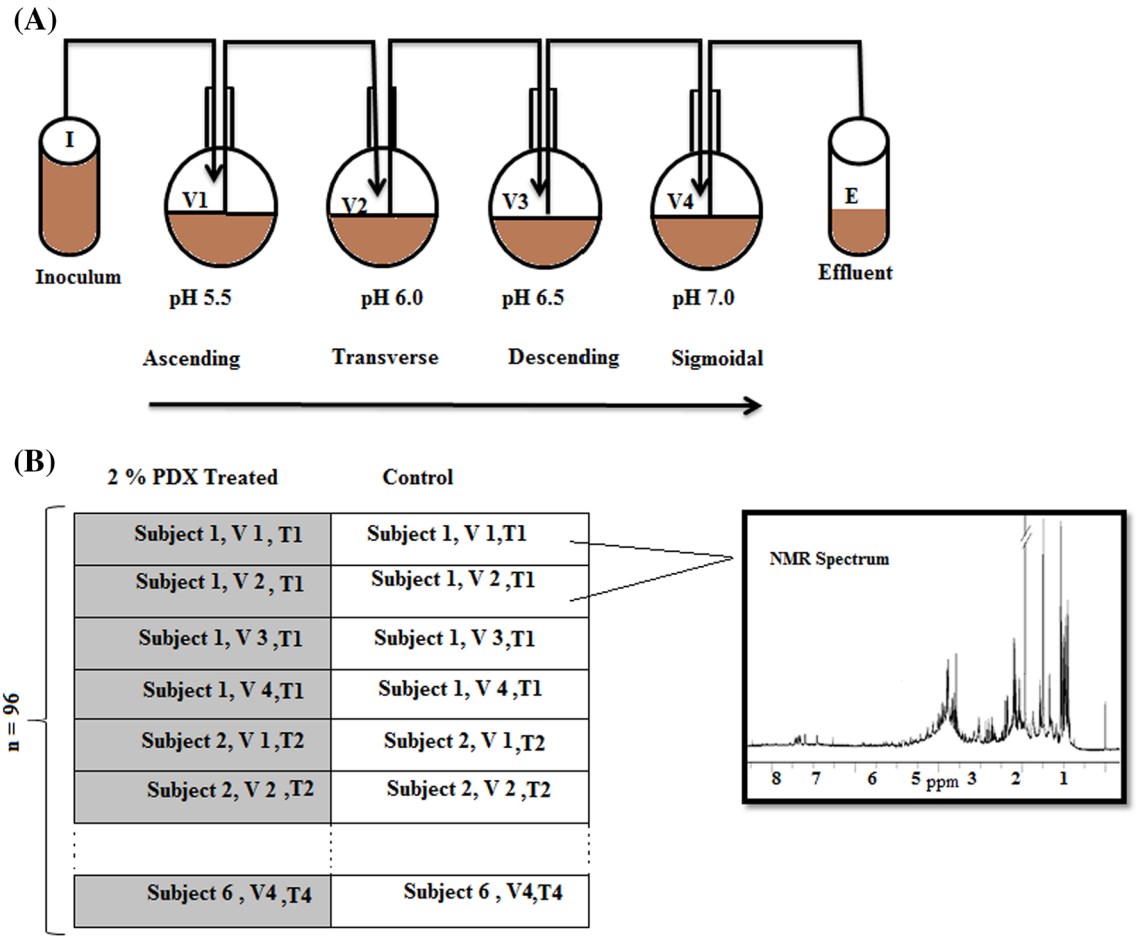

Fig. 1 The Enteromix model and the data set structure. **a** The vessels in one unit (V1–V4) simulate the different compartments of the human colon from proximal to the distal part, each having a different pH and flow rate. **b** The structure of dataset. In total 192 ($6_{\text{individual/simulation}} \times 4_{\text{vessels (V1–V4)}} \times 4_{\text{time points (T1 = 12, T2 = 24, T3 = 36,and T4 = 48 h)}} \times 2_{\text{with/without treatment}}$) samples were collected from the in vitro colon simulator. The dataset in this study has a paired structure (i.e. each PDX-treated sample has its own control)

related to dietary interactive modulations of the complex gut-microbe system.

Eminently, during the last decade metabolomics has emerged in the nutrition field with studies demonstrating the usefulness of untargeted metabolic profiling to improve the understanding of the complex relationships between diet and health (Deng et al. 2014; Garcia-Aloy et al. 2015; Pellis et al. 2012; Rezzi et al. 2007; Yde et al. 2014). Depending on different factors such as diet, environmental stress, and diseased condition, the metabolome of an individual may vary (Bundy et al. 2009; Emwas et al. 2013; Menni et al. 2013). These metabolic variations can be captured by an untargeted metabolic profiling approach which provides a mirror of the activity of the whole system. In this study we employed NMR-based metabolomics as a tool to characterize the impact of dietary fiber (i.e. PDX) on the in vitro derived fecal metabolome. Our aim was to examine the detailed dynamic metabolic changes occurring in different compartments of the colon simulator with and without PDX treatment.

2 Materials and methods

2.1 In vitro colon simulator

The Enteromix model of the human large intestine (Fig. 1a) has been described in details previously (Maki-vuokko et al. 2005). Briefly, this simulator consists of eight separate units, each containing four semi-continuously connected glass vessels. The vessels in one unit (V1–V4) model the different compartments of the human colon from the proximal to the distal part, each having a different pH and flow rate. In the initial phase of the simulation, each unit is inoculated with pre-incubated fecal microbes from a fresh faecal sample, which form the microbiota of the

colonic model. In the present study, the fecal samples for inoculum were provided voluntarily by six healthy Finnish volunteers (mean age 38.0 ± 8.3 years). Consequently, according to the Finnish law, no ethical approval is needed for this kind of study, since there has not been any interference with a person's physical or mental integrity. Within one simulation the fecal inoculum from one volunteer was used, and the system was fed in defined 3 h intervals synthetic ileal medium with/without 2 % PDX (Litesse Ultra; Danisco UK, Redhill, U.K.), i.e. all treated samples had their own control. This simulation was performed at Dupont Nutrition and Health, Kantvik, Finland. To understand the biochemical changes over time the microbial slurry was collected from all vessels (V1–V4) after 12, 24, 36, and 48 h with/without PDX treatment. In total 192 ($6_{\text{subjects}} \times 4_{\text{vessels (V1–V4)}} \times 4_{\text{time points (12, 24, 36, and 48 h)}} \times 2_{\text{ with/without treatment}}$) samples were collected from the in vitro colon simulator and stored at −80 °C prior to NMR analysis; the structure of dataset is depicted in Fig. 1b.

2.2 Preparation of simulated fecal water samples

Simulated fecal water was extracted with weight-to-buffer volume ratio of 1:1 in phosphate buffered saline (PBS, pH 7.4). The samples were homogenized by vortex mixing for 1 min, and then aliquots were centrifuged at 10,000×*g* for 10 min at 4 °C (Eppendorf 5471, USA). The supernatants were carefully removed and stored in Eppendorf tubes at −80 °C until analysis.

2.3 ^{1}H NMR spectroscopic analyses

Simulated fecal water samples extracted in PBS were thawed and centrifuged at 10,000×*g* for 10 min at 4 °C (Eppendorf 5471, USA). A volume of 500 µL of supernatant was transferred to a 5 mm NMR tube, and 100 µL of deuterium oxide (D_2O) containing 0.025 mg/mL of 3-trimethylsilyl propionic acid-*d*4 sodium salt (TSP) was added as a lock solvent. One-dimensional NMR

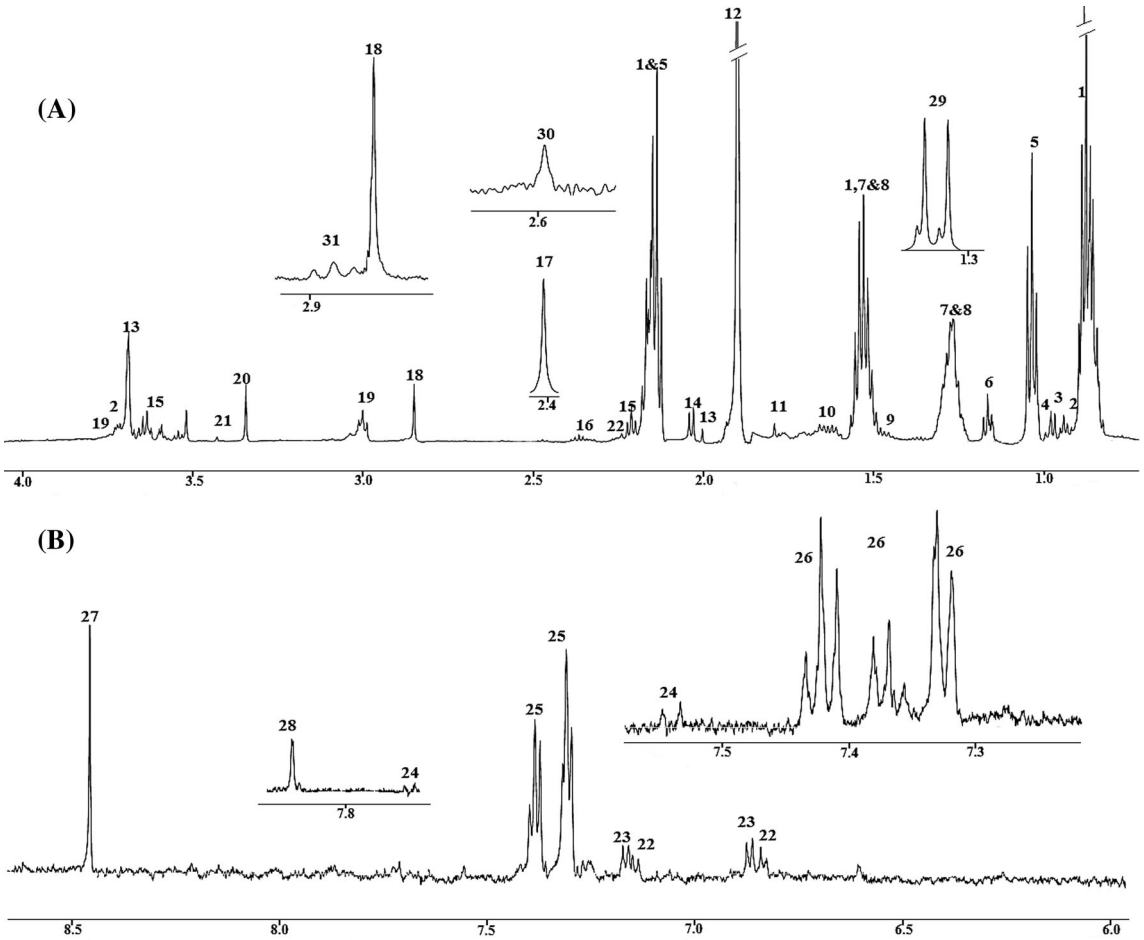

Fig. 2 Representative ^{1}H NMR spectrum of a simulated (Enteromix model) fecal sample extracted in PBS buffer. **a** 0.8–4.1 ppm; **b** 6–8.55 ppm. The aromatic region in the spectrum (6–8.55 ppm) has been magnified two times as compared to the aliphatic region (0.8–4.1 ppm). The inserts show additional signals detected in spectra obtained on other simulated fecal extract. Keys to the figure are given in Table 1

experiments were carried out using a Bruker Avance III 600 MHz spectrometer (Bruker, Rheinstetten, Germany) equipped with a 5 mm triple resonance (TXI) probe at 298 K. A noespr1d (90°-t_1-90°-d_{mix}-90°-FID, Bruker, Rheinstetten, Germany) pulse sequence with presaturation was performed to suppress signals from water molecules, where t_1 is a 4 µs delay time and d_{mix} is the mixing time. Acquisition parameters for the spectra were 64 scans, a spectral width of 7288 Hz collected into 32 K data points, an acquisition time of 2.24 s and a relaxation delay of 5 s. The Free Induction Decay (FID) obtained was multiplied by 0.3 Hz of line broadening before Fourier transformation. The spectra were referenced to TSP (chemical shift defined at 0 ppm), phased, and baseline corrected in Topspin 3.0 software (Bruker, Rheinstetten, Germany). Assignments of ^{1}H NMR signals were carried out using Chenomx NMR Suite 7.7 (Chenomx, Canada) according to the Human Metabolome Database and literature (Le Gall et al. 2011; Wishart et al. 2009). In addition, heteronuclear single quantum coherence (HSQC) 2D NMR was applied on selected samples to confirm the identity of the given metabolites. The HSQC experiment was acquired with a spectral width of 7288 Hz in the ^{1}H dimension and 27,164 Hz in the ^{13}C dimension, a matrix with a size of 2048 × 1024, 512 transients per increment and a relaxation delay of 2 s.

2.4 Multivariate data analysis

In total 192 NMR spectra were imported to MatlabR2010b (The Mathworks, Inc., USA). Misalignments of the spectra were corrected using the icoshift algorithm, based on the correlational shifting of spectral intervals (Savorani et al. 2010). The 8.5–12 ppm and −1.2 to 0.75 ppm regions and the region containing residual water resonance (4.7–4.8 ppm) were removed from the aligned spectra. The spectra were normalized to TSP signal and Pareto-scaled before multivariate modeling in MATLAB20010b (The Mathworks, Inc., USA). Principal component analysis (PCA) of the preprocessed NMR spectra (n = 192) was initially performed to visualize the general trend in the data using the PLS Toolbox 7.8 (Eigenvector Research, USA) in MATLAB2010b. Subsequently, multilevel simultaneous component analysis (MSCA) was performed exploiting the paired data structure in the experiment (Fig. 2) in order to explore the systematic variation between the PDX treated and the control samples. MSCA is an extension of PCA model that splits up the variation in the dataset into a between-subject part and a within-subject part (Jansen et al. 2005). Subsequently, supervised multilevel partial least square discriminant analysis (MLPLS-DA) was performed to discriminate between the PDX treated and control samples (n = 192). MLPLS-DA models were validated using double cross model validation (CMV) with twenty repeats. Permutation testing was carried out by randomly reassigning the class labels to the samples, to evaluate the statistical significance of the classification results. One thousand permutations were performed and the results were compared to the results of the original class labeling. p values ≤0.05 were considered significant. The algorithms for MSCA, MLPLS-DA, CMV, and permutation tests have been reported previously. (van Velzen et al. 2008; Yde et al. 2012). These algorithms are open access and available via the internet at http://www.bdagroup.nl/. To examine the metabolic changes over time (12, 24, 36, and 48 h) in the vessels (V1–V4), we subtracted the PDX treated spectra from the control spectra. The peak integration was performed using an in house built Matlab script (Matlab R20010b). Pearson's correlation coefficient between the integral of these metabolites was calculated in Matlab R20010b using statistical toolbox (The Mathworks, Inc., USA). The results are illustrated by heat maps (Matlab R20010b).

3 Results

The simulated fecal extract revealed a wide range of metabolites; predominantly SCFAs, branched chain fatty acids (BCFAs), organic acids, and amino acids. Figure 2 shows a representative ^{1}H NMR spectrum of a simulated fecal extract. A list of more than 30 identified resonances is given in Table 1.

3.1 Multivariate data analysis

To identify the metabolic impact of PDX in the in vitro colon simulation, multivariate data analysis (summarized is Table S2, supplementry information) was performed on the NMR spectra obtained from the simulated fecal extract (n = 192). PCA of the Pareto-scaled and normalized NMR spectra was performed to visualize general grouping and trends in the data. A notable effect of PDX treatment was observed on the NMR profile. The PCA score plot shows the PDX-treated samples mainly clustered in the direction of PC1 (Fig. 3a). From the loading (Fig. 3b) the clustering of the PDX treated samples along PC1 could mainly be ascribed to the presence of undigested PDX material (3.5–4.5 ppm) and oligomers of glucose (alpha anomeric protons) and other unidentified carbohydrates appearing in the spectral region of 5.0–5.5 ppm. Peak integrals of these residual PDX signals (3.5–4.5 ppm) depict that the level of PDX decreased during the time course (12, 24, 36, and 48 h) while passing from vessel V1–V4 (Supplementary Fig. S1). In addition, to focus on other, less dominating metabolite variations, PCA was also performed excluding

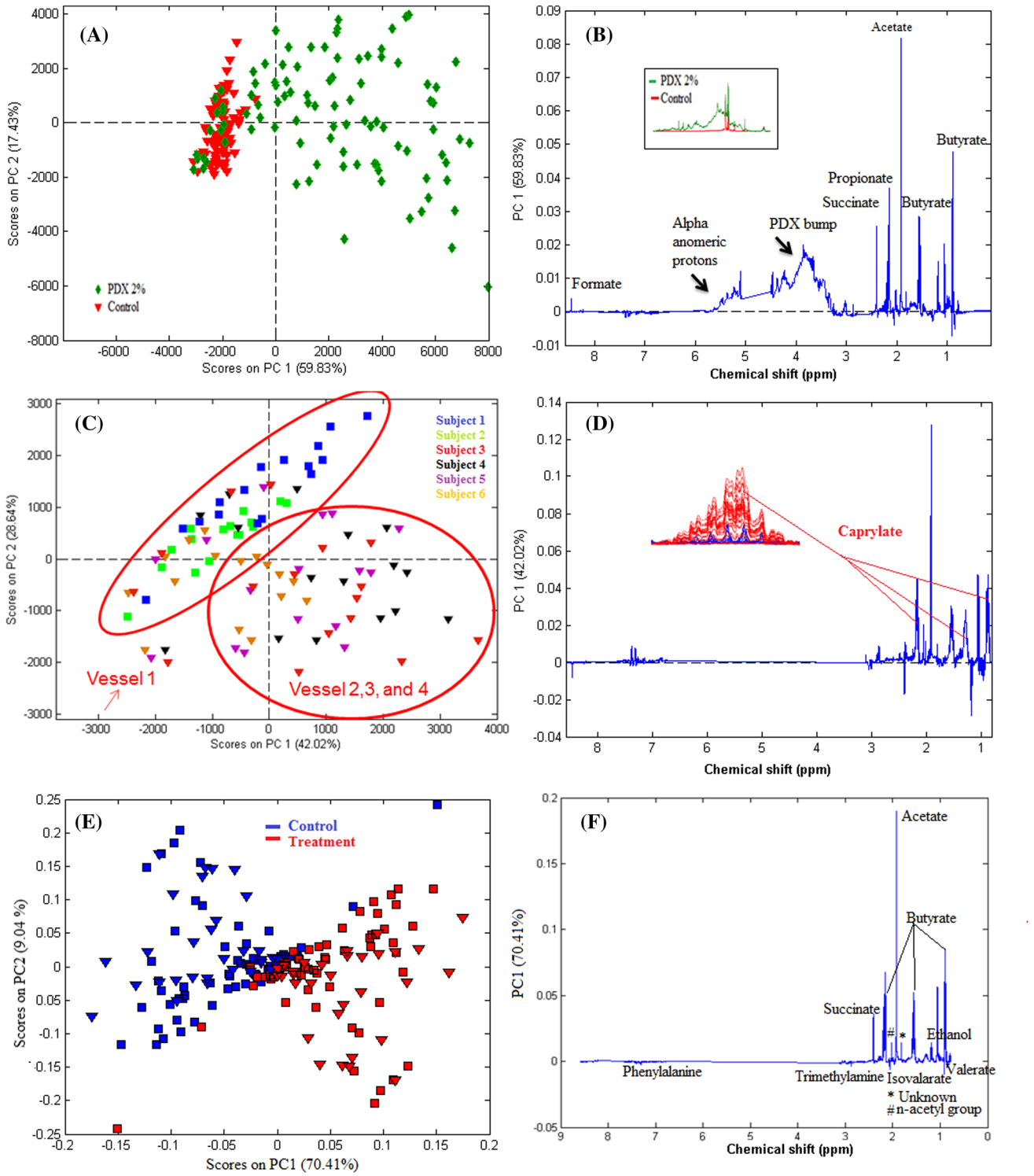

Fig. 3 Principal component analysis. **a** Score plot of the first and third principal component (PC) from 192 in vitro derived fecal samples *green diamond* PDX treated samples, *red inverted triangle* Control sample. **b** Loading profile of first principal component. The *inset* shows the mean spectral region (3.5–5.5 ppm) between PDX treated vs control samples. **c** Score plot of the first and second PC representing the between subject variation. Each color represents one of the six subjects included in the study; *square box* denotes subjects 1, and 2 while *triangle* represent subjects 3, 4, 5, and 6. The *red arrows* in the PC1 score plot denote subject 1, 2, 3 and 4 from vesse1 **d** Loading profile of first principal component. The corresponding loading plot and visual inspection of NMR spectra depicts that variation could predominantly be assigned to the signal from the caprylic acid (*Arrows* marked *red* in loading). **e** Score plot of the first and second PC representing the within-subject variation. The control and treated samples are colored coded accordingly **f** Loading profile of the first principal component of the within-subject variation (Color figure online)

3.5–5.5 ppm and 5.0–5.5 ppm region in the ^{1}H NMR spectra. It was apparent from the score and loading plots that metabolites varied between the samples with and without PDX; however, the clustering was ambiguous, which might be due to a sample-to-sample variation (data not shown). In order to minimize the sample-to-sample variation, multilevel data analysis was performed.

A multilevel approach exploits the paired data structure in the experiment (Westerhuis et al. 2010). MSCA was performed to split up the variation in the dataset into the between-subject part (biological variation) and the within-subject part (treatment effect). The MSCA analysis showed that a large proportion (42.02 %) of the between-subject variation could be described by PC1. The score plot in Fig. 3c shows that the NMR spectra from four out of six donors (colored coded) in vessel V2, V3, and V4 clustered together (circled red). The corresponding loading plot depicts that this variation could predominantly be assigned to signals from caprylic acid (1.27, 1.53, 2.16 ppm). Intriguingly, visual inspection of NMR spectra could disclose the same inter-individual variation in levels of caprylic acid (Fig. 3d). The result indicates that variation between subjects may be ascribed to different microbiota among the donors/individuals.

Furthermore, the within-subject model was examined to investigate if the PDX treatment induced any metabolic alterations. The results in Fig. 3e indicate that much of the within-subject variation was explained by PC1 (70.41 %). The score plot and loadings (Fig. 3e, f) of PDX-treated and control samples shows clear separation with PDX-treated samples having higher levels of butyrate, acetate, propionate, succinate, *N*-acetyl compound and an unidentified peak. On the other hand, control samples had higher levels of several amino acids (leucine, valine, isoleucine, phenylalanine, and lysine), valerate, isovalerate and trimethylamine compared to PDX-treated samples.

Multilevel PLS-DA was performed to further examine the metabolic effects of the PDX treatment on the simulated fecal metabolome. The multilevel PLS-DA model was validated by means of double cross model validation (CMV) to prevent over fitting of the multivariate model. (Szymanska et al. 2012, Westerhuis et al. 2010). The prediction error estimated in terms of number of misclassifications based on 20 CMV repeats showed on average 26.1 samples predicted incorrectly, which account for about 13.5 % of all the prediction results. The permutation results indicated this to be a significant result. Moreover, the area under the receiver operating characteristic (AUROC = 0.92) also reflects that the ability of discrimination model to correctly classify the samples with and without PDX treatment were excellent. Importantly, the regression coefficient plot showed that the most differentiating metabolites between the PDX treated and control samples were similar to those obtained from the MSCA model (Supplementary information, Fig. S2). Thus, these results signify the higher levels of butyrate, acetate, propionate, succinate, *N*-acetyl compound and lower levels of amino acids (leucine, valine, isoleucine, phenylalanine, tyrosine and lysine), valerate, isovalerate and trimethylamine among the PDX treated samples when compared to the control samples.

3.2 Biochemical changes in the colon simulator

Besides exploring the impact of PDX on the in vitro generated metabolome, our objective was to understand the dynamic metabolic/biochemical changes occurring in different compartments of the colon simulator over time. In order to examine the metabolic changes over time (12, 24, 36, and 48 h) in the vessels (V1–V4) comprehensively, we subtracted the PDX treated spectra from the control spectra. Peak integrals of SCFAs (acetate, butyrate, and propionate), branched chain fatty acids (iso-valerate), biogenic amine (trimethylamine), organic metabolites (succinate, ethanol, formate, valerate, and n-acetyl compound) and amino acids (lysine, leucine, iso-leucine, phenylalanine, tyrosine, and valine) were obtained from the subtracted matrix and plotted accordingly. The Fig. 5 depicts the metabolic changes of alanine, succinate, *N*-acetyl compound and butyrate from six simulations/subjects in four vessels (V1–V4) over four time points (12, 24, 36, and 48 h).

Based on the results from our study, the time course change of the metabolites in the vessels of the in vitro simulator could be summarized according to their observed trends. The level of alanine in vessel (V1–V4) decreased over the time course (12, 24, 36, and 48 h) with higher level of variation appearing in the vessel V_1 over time and within subjects (Fig. 4a). Intriguingly, all others amino acids (lysine, leucine, isoleucine, and valine), ethanol, isovalerate, and trimethylamine showed similar trend in the entire vessel over time (Supplementary information, Fig. S3). Succinate (Fig. 4b) and formate (Supplementary information, Fig. S3) had a unique progression pattern as they mainly appeared in vessel V1 and V2. Intriguingly, visual inspection of NMR spectra showed that five out of six individuals exclusively had succinate in the PDX-treated sample.

On the other hand, the levels of an *N*-acetyl compound (Fig. 4c) and butyrate (Fig. 4d) gradually increased in the four vessels (V1–V4) over four time points (12, 24, 36, and 48 h) which was also the general pattern for acetate (Supplementary information, Fig. S3) and unknown peak at 1.82 ppm (data not shown). Interestingly, the level of residual PDX (data not shown) also showed a similar trend to that of the *N*-acetyl compound. The correlation analysis

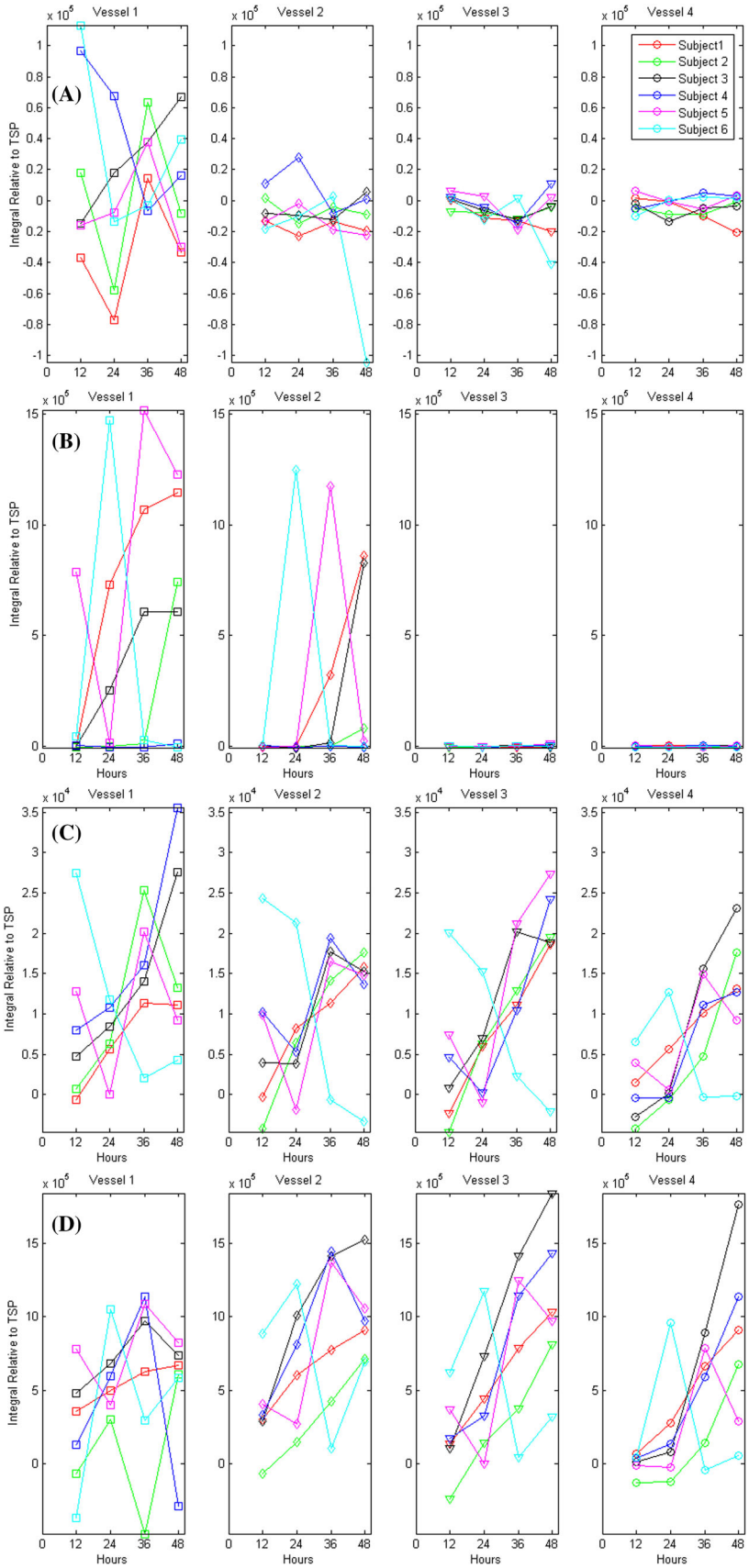

Fig. 4 The figure depicts the metabolic changes from six simulation/donors in four vessels (V1–V4) over four time points (12, 24, 36, and 48 h). Each color in the figure represents the individual donors for the simulation. **a** Alanine, **b** succinate, **c** *N*-acetyl compound, and **d** butyrate

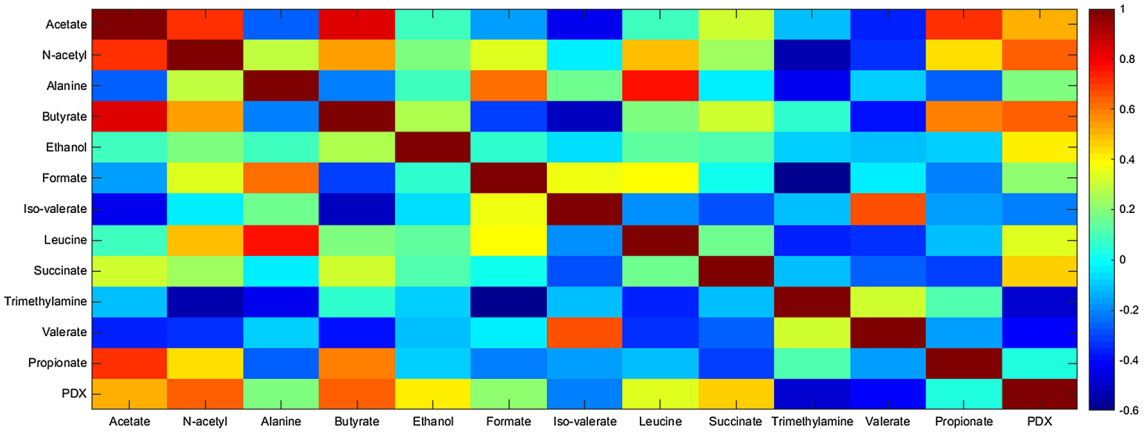

Fig. 5 Correlation coefficients illustrated by heat map. The Pearson correlation coefficient (R) value revealed that the PDX level in the vessels were positively correlated with the *N*-acetyl compound, acetate, propionate butyrate, ethanol, formate, leucine, succinate, but negatively correlated with iso-valarate, valerate, and trimethylamine. The color-coding in the figure represents the R values

between the level of all metabolites and PDX was performed to explore the inter-variable correlations (Fig. 5). The PDX levels in the vessel were positively correlated with the *N*-acetyl compound, acetate, propionate, butyrate, ethanol, formate, leucine, and succinate while negatively correlated with iso-valarate, valerate, and trimethylamine. However, the highest statistical associations ($p < 0.05$) were observed for *N*-acetyl compound, acetate, butyrate, succinate, valerate, and trimethylamine. Thereby, correlation coefficient analysis enabled us to identify the potential associations between the level of residual PDX and other metabolites in the in vitro colon simulator.

4 Discussion

Dietary fibers and prebiotics are considered to play an important role in human health and there is an increasing interest in evaluating the impact of dietary fibers on the complex gut system. The objective of the current study was to evaluate the impact of PDX; a soluble dietary fiber in the in vitro simulator using untargeted and dynamic NMR metabolic profiling. NMR based metabolomics allowed us to explore a wide range of metabolites present in the in vitro derived fecal material, and the PDX-induced metabolite changes in the in vitro simulator could be investigated more comprehensively than in previous targeted studies (Makivuokko et al. 2005, 2007).

A recent study on fecal metabolomics after human intervention trial disclosed a strong effect of PDX intake due to the presence of residual PDX and unknown oligosaccharides in the feces (Lamichhane et al. 2014). Similar results were obtained in the current study, as PDX-treated samples were distinct from control samples due to the presence of undigested PDX (3.5–4.5 ppm) and depolymerized products of PDX (5.0–5.5 ppm, Fig. 3a, b). We observed distinct changes in the level of the PDX and depolymerized products of PDX while passing from vessel (V1–V4) over four times (12, 24, 36, and 48 h). Moreover, the presence of oligomers of glucose (5.0–5.5 ppm) in the vessels (V1–V4) provides evidence of the ongoing saccharolytic activity by the colonic microbiota in the simulator. Consequently, the present findings indicate that metabolism of PDX sets in the proximal colon (V1) and fermentation continues until the distal part of the colon (V4) (Makelainen et al. 2007). In fact, carbohydrate fermentation has been identified as the most important driving force to regulate the metabolic activities in the colon. The rate of de-polymerization of the carbohydrates and availability of these products particularly in the distal colon are linked with colonic health/disease (Macfarlane et al. 1992; Macfarlane and Macfarlane 2012). Based on our finding it may thus be suggested that availability of PDX as substrate for fermentation in the distal colon is associated with a potential health benefit. However, this proposed hypothesis requires further substantiation in terms of metabolic activity of microbiota in the colon regarding the undigested PDX and depolymerized products of PDX.

To characterize the complete metabolic effects of PDX digestion by the microbiota in the in vitro gut metabolome, multilevel data analysis showed that the inter-individual variation could be predominantly linked to the presence of caprylic acid among the subjects. Caprylic acid, which is a medium chain fatty acid, is considered a side-product from sugar fermentation and is mostly derived from acetate (Steinbusch et al. 2011). Earlier studies have indicated an antibacterial and antifungal effect of caprylic acid (Corsetti et al. 1998; Skrivanova et al. 2008). Interestingly, Corsetti et al. showed that lactic acid bacteria produce caprylic acid (Corsetti et al. 1998). However, it remains unknown if this

compound is produced by lactic acid bacteria alone, as it might also be produced by numerous other strains through the colon (Lemfack et al. 2014). Therefore, we suggest that the identified variability in the metabolic end product is due to the difference in microbial composition between the individuals as previously hypothesized.

In the present study, in addition to inter-individual variation, we evaluated if PDX treatment modulated the in vitro derived fecal metabolite profile. We observed higher levels of butyrate, acetate, propionate, succinate, *N*-acetyl compound and lower level of amino acids (leucine, valine, isoleucine, phenylalanine, and lysine), valerate, formate, isovalerate and trimethylamine among the PDX-treated samples when compared to the control samples. Our result is in agreement with previous reports from animal models, in vitro models, and humans showing that PDX intake increases the production of SCFA, in particular butyrate, propionate, and acetate (Beloshapka et al. 2012; Figdor and Rennhard 1981; Jie et al. 2000; Makivuokko et al. 2005). On the contrary, some studies did not detect any significant change in SCFAs level due to PDX fermentation (Costabile et al. 2012; Lamichhane et al. 2014). This discrepancy in the in vivo results might be affected, by many confounding factors connected to diet and lifestyle, which is challenging to standardize. However, an in vitro study has more controlled experimental conditions compared to an in vivo experiment which consequently results in lower inter and intra sample variation. Therefore in vitro models may be advantageous to test and exploit hypotheses regarding the impact of food components/drugs on the human gut system. In fact SCFAs, primarily acetate, propionate, and butyrate, are end products of fermentation of complex carbohydrates such as dietary fiber (Macfarlane and Macfarlane 2012). The amount of SCFAs production primarily depends on the availability of substrates and the diversity of microbiota present in the colon (Besten et al. 2013; Macfarlane and Macfarlane 2003). Even though acetate is the principal SCFA in the colon, butyrate is of particular interest because it is the major energy source for colonocytes and has vital role in prevention of colon related disease particularly in the distal colon (Hamer et al. 2008). Our result depicts higher level of butyrate in the four vessels (V1–V4) over four time points (12, 24, 36, and 48 h) in the PDX treated samples. Therefore, increases in SCFA production, specifically butyrate, due to PDX digestion in the distal colon may eventually maximize the colonic disease prevention.

In addition to SCFAs variation, we observed that succinate and *N*-acetyl compound were elevated in the PDX-treated samples. Succinate is also a common end product formed by certain groups of bacteria under specific environment condition. The decarboxylation of succinate produces propionate in the gut (Macfarlane and Macfarlane 2003). Interestingly, studies have shown that when sufficient carbohydrate is present during bacterial metabolism, there is a reduced need for succinate decarboxylation and as result succinate is accumulated instead (Macfarlane and Macfarlane 2003; Macy et al. 1978). Our results demonstrated a similar finding, thus providing substantial evidence for regulation of biosynthetic pathways of the major microbial metabolite, specifically succinate and propionate as a result of carbohydrate fermentation. Furthermore, this finding is also supported by a strong negative correlation between propionate and succinate (Fig. 5). To the best of our knowledge, this is first study to show that *N*-acetyl compound was elevated in the PDX-treated samples. This is an intriguing finding as *N*-acetyl compound, in particular n-acetyl glucosamine; receive considerable attention due to its therapeutic potential in inflammatory bowel disease (Kamel and Alnahdi 1992; Liu et al. 2013; Salvatore et al. 2000). Even though a conclusive proof for these indications is not available, our data suggest that increased level of *N*-acetyl compound due to PDX digestion might be linked to possible digestive health benefits. Thus, our finding calls for further studies to explore possible the link between PDX fermentation, *N*-acetyl compound, and its role in the regulation of gut health.

The lower levels of amino acids, BCFA (isovalerate) and biogenic amine (trimethylamine) in the PDX-treated samples that were identified in the present study indicate an ongoing sustained saccharolytic activity in the simulator. Sustained saccharolytic activity has been associated with reduced putrefaction or/and proteolytic activities in the colon (Macfarlane et al. 1992; Macfarlane and Macfarlane 2003). More specifically, depletion of readily available carbohydrate for fermentation may induce proteolytic activity, which is considered an alternative pathway for carbon, nitrogen, and an energy source for the microbes in the colon. As result, not only SCFAs but also toxic compounds such as indoles, biogenic amine, phenols, and thiols are produced during putrefaction (Cummings and Macfarlane 1991; Smith and Macfarlane 1997a, b). Large amounts of these toxic end products have been linked with a detrimental effect on the colon health (Smith and Macfarlane 1997a, b). Intriguingly, our data indicate reduced levels of amino acids, BCFA, and biogenic amine due to PDX fermentation in the in vitro colon simulation model. This finding is potentially of metabolic significance, since the majority of toxin formations and colon diseases have been associated with putrefaction. Meanwhile, it is also noteworthy that negative correlations observed between PDX and amino acids, isovalerate, and trimethylamine in four vessels (V1–V4) over four time points (12, 24, 36, and 48 h) further strengthen the metabolic significance of PDX in the colon simulator (Fig. 5). Consequently, it may be suggested that sustained PDX fermentation in the in vitro

colon simulation (vessels V1–V4) is associated with a reduction in proteolytic activity in the colon, which thereby contributes to an improved gut health.

5 Conclusion

Overall, our study shows that the combination of NMR based metabolomics and multivariate data analysis enabled us to characterize the impact of PDX on the in vitro derived fecal metabolome more comprehensively than in previous targeted studies. Importantly, multilevel data analysis improved the interpretability of the multivariate model by decomposing the variation into between and within subject sub-models. Despite substantial inter-individual variation in the composition of the metabolites, our study based on in vitro simulator experiments has shown that PDX fermentation has substantial effects on the in vitro derived faecal metabolome. These effects are detectable already in vessel V1 where fermentation of PDX begins and continues to vessel V4 in the colon simulator. Beneficial metabolic effects of PDX were indicated by the presence of higher levels of butyrate, acetate, propionate, *N*-acetyl compound and lower levels of amino acids, BCFA, and trimethylamine in the PDX-treated samples. In future, our work may provide a useful approach to understand the metabolic impact of potential prebiotic compounds and get deep insight into the molecular regulation of gut-microbes interaction in the gut.

Acknowledgments The present study is part of the Ph.D. work of Santosh Lamichhane and was financially supported by DuPont, Food Future Innovation (FFI), and Aarhus University.

Complaince with ethical standards

Conflict of interest The authors declare that they have no competing interests.

Ethical statement The fecal samples used as inoculum in the colon simulator were given voluntarily by six healthy Finnish volunteers. According to the Finnish law, no ethical approval is needed for this kind of study, since there has not been any interference with a person's physical or mental integrity.

References

Achour, L., Flourié, B., Briet, F., Pellier, P., Marteau, P., & Rambaud, J. C. (1994). Gastrointestinal effects and energy value of polydextrose in healthy nonobese men. *American Journal of Clinical Nutrition, 59*, 1362–1368.

Beloshapka, A. N., Wolff, A. K., & Swanson, K. S. (2012). Effects of feeding polydextrose on faecal characteristics, microbiota and fermentative end products in healthy adult dogs. *British Journal of Nutrition, 108*, 638–644.

Bundy, J., Davey, M., & Viant, M. (2009). Environmental metabolomics: A critical review and future perspectives. *Metabolomics, 5*, 3–21.

Corsetti, A., Gobbetti, M., Rossi, J., & Damiani, P. (1998). Antimould activity of sourdough lactic acid bacteria: Identification of a mixture of organic acids produced by Lactobacillus sanfrancisco CB1. *Applied Microbiology and Biotechnology, 50*, 253–256.

Costabile, A., et al. (2012). Impact of polydextrose on the faecal microbiota: A double-blind, crossover, placebo-controlled feeding study in healthy human subjects. *British Journal of Nutrition, 108*, 471–481.

Cummings, J. H., & Macfarlane, G. T. (1991). The control and consequences of bacterial fermentation in the human colon. *Journal of Applied Bacteriology, 70*, 443–459.

den Besten, G., van Eunen, K., Groen, A. K., Venema, K., Reijngoud, D.-J., & Bakker, B. M. (2013). The role of short-chain fatty acids in the interplay between diet, gut microbiota, and host energy metabolism. *Journal of Lipid Research, 54*, 2325–2340.

Deng, P., Jones, J., & Swanson, K. (2014). Effects of dietary macronutrient composition on the fasted plasma metabolome of healthy adult cats. *Metabolomics, 10*, 638–650.

Emwas, A.-H., Salek, R., Griffin, J., & Merzaban, J. (2013). NMR-based metabolomics in human disease diagnosis: Applications, limitations, and recommendations. *Metabolomics, 9*, 1048–1072.

Figdor, S. K., & Rennhard, H. H. (1981). Caloric utilization and disposition of [14C] polydextrose in the rat. *Journal of Agricultural and Food Chemistry, 29*, 1181–1189.

Garcia-Aloy, M., et al. (2015). Nutrimetabolomics fingerprinting to identify biomarkers of bread exposure in a free-living population from the PREDIMED study cohort. *Metabolomics, 11*, 155–165.

Hamer, H. M., Jonkers, D., Venema, K., Vanhoutvin, S., Troost, F. J., & Brummer, R. J. (2008). Review article: The role of butyrate on colonic function. *Alimentary Pharmacology & Therapeutics, 27*, 104–119.

Hernot, D. C., et al. (2009). In vitro fermentation profiles, gas production rates, and microbiota modulation as affected by certain fructans, galactooligosaccharides, and polydextrose. *Journal of Agricultural and Food Chemistry, 57*, 1354–1361.

Hull, S., Re, R., Tiihonen, K., Viscione, L., & Wickham, M. (2012). Consuming polydextrose in a mid-morning snack increases acute satiety measurements and reduces subsequent energy intake at lunch in healthy human subjects. *Appetite, 59*, 706–712.

Jansen, J. J., Hoefsloot, H. C. J., van der Greef, J., Timmerman, M. E., & Smilde, A. K. (2005). Multilevel component analysis of time-resolved metabolic fingerprinting data. *Analytica Chimica Acta, 530*, 173–183.

Jie, Z., et al. (2000). Studies on the effects of polydextrose intake on physiologic funtions in Chinese people. *American Journal of Clinical Nutrition, 72*, 1503–1509.

Kamel, M., & Alnahdi, M. (1992). Inhibition of superoxide anion release from human polymorphonuclear leukocytes by *N*-acetyl-galactosamine and *N*-acetyl-glucosamine. *Clinical Rheumatology, 11*, 254–260.

Lahtinen, S. J., et al. (2010). Effect of molecule branching and glycosidic linkage on the degradation of polydextrose by gut microbiota. *Bioscience, Biotechnology, and Biochemistry, 74*, 2016–2021.

Lamichhane, S., et al. (2014). Impact of dietary polydextrose fiber on the human gut metabolome. *Journal of Agriculture and Food Chemistry, 62*, 9944–9951.

Le Gall, G., et al. (2011). Metabolomics of fecal extracts detects altered metabolic activity of gut microbiota in ulcerative colitis and irritable bowel syndrome. *Journal of Proteome Research, 10*, 4208–4218.

Lemfack, M. C., Nickel, J., Dunkel, M., Preissner, R., & Piechulla, B. (2014). mVOC: A database of microbial volatiles. *Nucleic Acids Research, 42*, D744–D748.

Liu, L., et al. (2013). Microbial production of glucosamine and *N*-acetylglucosamine: Advances and perspectives. *Applied Microbiology and Biotechnology, 97*, 6149–6158.

Macfarlane, G. T., Gibson, G. R., & Cummings, J. H. (1992). Comparison of fermentation reactions in different regions of the human colon. *Journal of Applied Bacteriology, 72*, 57–64.

Macfarlane, S., & Macfarlane, G. T. (2003). Regulation of short-chain fatty acid production. *Proceedings of the Nutrition Society, 62*, 67–72.

Macfarlane, G. T., & Macfarlane, S. (2012). Bacteria, colonic fermentation, and gastrointestinal health. *Journal of AOAC International, 95*, 50–60.

Macy, J. M., Ljungdahl, L. G., & Gottschalk, G. (1978). Pathway of succinate and propionate formation in Bacteroides fragilis. *Journal of Bacteriology, 134*, 84–91.

Makelainen, H. S., Makivuokko, H. A., Salminen, S. J., Rautonen, N. E., & Ouwehand, A. C. (2007). The effects of polydextrose and xylitol on microbial community and activity in a 4-stage colon simulator. *Journal of Food Science, 72*, M153–M159.

Makivuokko, H., Nurmi, J., Nurminen, P., Stowell, J., & Rautonen, N. (2005). In vitro effects on polydextrose by colonic bacteria and caco-2 cell cyclooxygenase gene expression. *Nutrition and Cancer, 52*, 94–104.

Mäkivuokko, H., et al. (2007). The effect of cocoa and polydextrose on bacterial fermentation in gastrointestinal tract simulations. *Bioscience, Biotechnology, and Biochemistry, 71*, 1834–1843.

Menni, C., et al. (2013). Targeted metabolomics profiles are strongly correlated with nutritional patterns in women. *Metabolomics, 9*, 506–514.

Mills, C. E., Tzounis, X., Oruna-Concha, M. J., Mottram, D. S., Gibson, G. R., & Spencer, J. P. (2015). In vitro colonic metabolism of coffee and chlorogenic acid results in selective changes in human faecal microbiota growth. *British Journal of Nutrition,*. doi:10.1017/S0007114514003948.

Nicholson, J. K., et al. (2012). Host-gut microbiota metabolic interactions. *Science, 336*, 1262–1267.

Pellis, L., et al. (2012). Plasma metabolomics and proteomics profiling after a postprandial challenge reveal subtle diet effects on human metabolic status. *Metabolomics, 8*, 347–359.

Pereira-Caro, G., et al. (2015). In vitro colonic catabolism of orange juice (poly)phenols. *Molecular Nutrition & Food Research, 59*, 465–475.

Rezzi, S., Ramadan, Z., Fay, L. B., & Kochhar, S. (2007). Nutritional metabonomics: Applications and perspectives. *Journal of Proteome Research, 6*, 513–525.

Roberfroid, M., et al. (2010). Prebiotic effects: Metabolic and health benefits. *British Journal of Nutrition, 104*(Suppl 2), S1–S63.

Romick-Rosendale, L., Legomarcino, A., Patel, N., Morrow, A., & Kennedy, M. (2014). Prolonged antibiotic use induces intestinal injury in mice that is repaired after removing antibiotic pressure: Implications for empiric antibiotic therapy. *Metabolomics, 10*, 8–20.

Ryan, D., Newnham, E., Prenzler, P., & Gibson, P. (2014). Metabolomics as a tool for diagnosis and monitoring in coeliac disease. *Metabolomics,*. doi:10.1007/s11306-014-0752-9.

Salvatore, S., et al. (2000). A pilot study of *N*-acetyl glucosamine, a nutritional substrate for glycosaminoglycan synthesis, in paediatric chronic inflammatory bowel disease. *Alimentary Pharmacology & Therapeutics, 14*, 1567–1579.

Savorani, F., Tomasi, G., & Engelsen, S. B. (2010). icoshift: A versatile tool for the rapid alignment of 1D NMR spectra. *Journal of Magnetic Resonance, 202*, 190–202.

Skrivanova, E., Molatova, Z., & Marounek, M. (2008). Effects of caprylic acid and triacylglycerols of both caprylic and capric acid in rabbits experimentally infected with enteropathogenic *Escherichia coli* O103. *Veterinary Microbiology, 126*, 372–376.

Smith, E. A., & Macfarlane, G. T. (1997a). Dissimilatory amino acid metabolism in human colonic bacteria. *Anaerobe, 3*, 327–337.

Smith, E. A., & Macfarlane, G. T. (1997b). Formation of phenolic and indolic compounds by anaerobic bacteria in the human large intestine. *Microbial Ecology, 33*, 180–188.

Steinbusch, K. J. J., Hamelers, H. V. M., Plugge, C. M., & Buisman, C. J. N. (2011). Biological formation of caproate and caprylate from acetate: Fuel and chemical production from low grade biomass. *Energy & Environmental Science, 4*, 216–224.

Szymańska, E., Saccenti, E., Smilde, A. K., & Westerhuis, J. A. (2012). Double-check: validation of diagnostic statistics for PLS-DA models in metabolomics studies. *Metabolomics, 8*, 3–16.

van Velzen, E. J., et al. (2008). Multilevel data analysis of a crossover designed human nutritional intervention study. *Journal of Proteome Research, 7*, 4483–4491.

Westerhuis, J. A., van Velzen, E. J., Hoefsloot, H. C., & Smilde, A. K. (2010). Multivariate paired data analysis: Multilevel PLSDA versus OPLSDA. *Metabolomics, 6*, 119–128.

Wishart, D. S., et al. (2009). HMDB: A knowledgebase for the human metabolome. *Nucleic Acids Research, 37*, D603–D610.

Yde, C. C., Westerhuis, J. A., Bertram, H. C., & Bach Knudsen, K. E. (2012). Application of NMR-based metabonomics suggests a relationship between betaine absorption and elevated creatine plasma concentrations in catheterised sows. *British Journal of Nutrition, 107*, 1603–1615.

Yde, C., et al. (2014). Multi-block PCA and multi-compartmental study of the metabolic responses to intake of hydrolysed versus intact casein in C57BL/6J mice by NMR-based metabolomics. *Metabolomics, 10*, 938–949.